Green's function embedding using sum-over-pole representations

Andrea Ferretti [1,*] Tommaso Chiarotti [2] and Nicola Marzari [2,3]
[1]*Centro S3, CNR–Istituto Nanoscienze, 41125 Modena, Italy*
[2]*Theory and Simulations of Materials (THEOS) and National Centre for Computational Design and Discovery of Novel Materials (MARVEL), École Polytechnique Fédérale de Lausanne, 1015 Lausanne, Switzerland*
[3]*Laboratory for Materials Simulations (LMS), Paul Scherrer Institut (PSI), 5232 Villigen PSI, Switzerland*

(Received 12 September 2023; revised 10 April 2024; accepted 11 April 2024; published 29 July 2024)

In Green's function theory, the total energy of an interacting many-electron system can be expressed in a variational form using the Klein or Luttinger-Ward functionals. Green's function theory also naturally addresses the case where the interacting system is embedded into a bath. The latter can then act as a dynamical (i.e., frequency-dependent) potential, providing a more general framework than that of conventional static external potentials. Notably, the Klein functional includes a term of the form $\mathrm{Tr}_\omega \ln\{G_0^{-1}G\}$, where Tr_ω is the integration in frequency of the trace operator. Here, we show that using a sum-over-poles representation for the Green's functions and the algorithmic-inversion method one can obtain, in full generality, an explicit analytical expression for $\mathrm{Tr}_\omega \ln\{G_0^{-1}G\}$. Further, this allows us (1) to recover an explicit expression for the random phase approximation correlation energy in the framework of the optimized effective potential and (2) to derive a variational expression for the Klein functional valid in the presence of an embedding bath.

DOI: 10.1103/PhysRevB.110.045149

I. INTRODUCTION

Electronic-structure simulations based on density-functional theory (DFT) [1] are today widely exploited [2] in condensed-matter physics, quantum chemistry, and materials simulations [3]. Even if DFT can, in principle, be used to access any observable of an interacting system as a functional of the density [3–5], currently available functionals and approximations are mostly limited to the ground-state total energy (and, in turn, to its derivatives with respect to external parameters) and to observables connected to the charge density. Instead, electronic excitations can be addressed by extensions of the basic theory, such as time-dependent (TD) DFT [6–8] and ensemble DFT [9–11]. All these approaches are equipped with a variational principle which allows one to determine the basic quantity of the theory (e.g., the density in DFT or its time-dependent version in TD-DFT [12]) for the systems studied.

Conversely, Green's function (GF) methods [5,13] such as the GW approximation and its combination with the Bethe-Salpeter equation [14–17] are commonly used to address charged and neutral excitations. Nevertheless, the one-particle GF can also be used to access the ground-state total energy [5,18] (e.g., via the Galitskii-Migdal expression). A variational formulation with respect to the one-particle Green's function can be recovered by using the Luttinger-Ward and Klein energy functionals [19–22], which become stationary when evaluated at the interacting Green's function of the system. Applications have covered atoms and molecules [23–26], Hubbard chains [27,28], and the homogeneous electron gas [29–31]. When the Klein functional is combined with an optimized effective potential approach [32,33], one obtains the linearized Sham-Schlüter equation [34,35], which can be used to derive advanced Kohn-Sham DFT functionals from diagrammatic approximations, such as the exact exchange plus RPA exchange-correlation functional [5,13,18,22,36–39]. Notably, the Klein functional features a term of the form $\int \frac{d\omega}{2\pi i}\mathrm{Tr}\ln\{G_0^{-1}G\}$ (see Sec. II for more details), which is cumbersome to evaluate numerically and requires dedicated treatment [26,27]. The Luttinger-Ward functional displays similar issues. In passing, we also note that besides DFT-based and GF methods, other orbital-dependent or dynamical approaches [3] addressing excitations are available; these include dynamical mean-field theory (DMFT) [40], spectral potentials [41,42], and Koopmans-compliant functionals [42–45].

Importantly, dynamical potentials naturally emerge in the description of embedding, where a system of interest is placed in contact with an external bath. In these cases, for noninteracting systems, the embedded GF can be calculated by adding an embedding self-energy [5,13], which has the form of a nonlocal and dynamical potential, to the pristine Hamiltonian. This approach has been successfully exploited, e.g., in the description of semi-infinite systems (surface Green's function) and applied to simulations of quantum transport through nanojunctions [46–50]. When electron-electron interactions are considered, the situation becomes more complex, but the assumption of dealing with a noninteracting bath [46] allows one to treat the problem similarly to the noninteracting case. Approaches such as DMFT [40], which is a dynamical method targeting both total energies and spectral properties, exploit the embedding of an interacting impurity model to describe the electron-electron self-energy of strongly interacting systems.

*Corresponding author: andrea.ferretti@nano.cnr.it

In general, the use of dynamical potentials (e.g., originating from many-body perturbation theory [5,13], embedding, or spectral potentials [3,41,42]) in electronic-structure methods is a challenge by itself. Indeed, the frequency representation of propagators (or dynamical potentials) is nontrivial [31,51,52], with viable approaches ranging from discretized frequency grids (on either the real or imaginary axis) to the use of meromorphic functions and Padé approximants [53,54] or imaginary-time treatments [54]. Moreover, the solution of the resulting Dyson equation (which can be cast in the form of a nonlinear eigenvalue problem [55]) adds further numerical and conceptual complexity (including multiple solutions and nonorthonormality of the eigenvectors [5,16,55]). In order to address this problem, we recently combined a sum-over-poles (SOP) representation of the propagators with the algorithmic-inversion method (AIM) [31,51,52] to exactly solve the Dyson equation in the presence of dynamical potentials. In the context of GW calculations, a SOP formulation has also been used recently in the multipole approximation (MPA) method [56,57] to represent the frequency dependence of the response function in order to go beyond the plasmon-pole approach.

In this work, by taking advantage of the AIM-SOP formulation [31,51,52], we first derive an analytical expression for terms of the form $\mathrm{Tr}_\omega\{G_0^{-1}G\}$, appearing, e.g., in the Klein functional, which is valid in the general case of interacting propagators. Next, we exploit this result (1) to recover an exact expression [36] for the random phase approximation (RPA) correlation energy [22,38,39] and (2) to obtain a Klein functional valid in the case of embedding where the system of interest is coupled to a noninteracting bath. Furthermore, in Appendix A 1 we also derive a dynamical noninteracting v-representability condition for the Green's function of the system.

This paper is organized as follows. In Sec. II we present the theoretical framework used throughout the work. Next, in Sec. III we derive an analytical expression for $\mathrm{Tr}_\omega\{G_0^{-1}G\}$. Finally, in Sec. IV we apply the result derived to evaluate the RPA correlation energy first, and then to obtain the embedding of the Klein functional. Complementary details about Green's function embedding and Trln terms are provided in Appendixes A and B, respectively.

II. THEORETICAL FRAMEWORK

In this section we present the theoretical framework underpinning the use of Green's function methods to describe an interacting system in the presence of a noninteracting bath; additional details are provided in Appendix A. We consider a closed quantum system C that is partitioned into two subsystems, the interacting system S and the bath B, such that, in terms of degrees of freedom, we have $C = S \cup B$. Particle interactions are present but limited to only subsystem S, leaving subsystem B as a noninteracting bath. All single-particle operators, including Hamiltonians, self-energies, and the Green's function, become 2×2 block matrices, indexed according to the S and B subsystems. As detailed in Fig. 1, h_0 represents the noninteracting Hamiltonian of the two systems without coupling, while H_0 is the noninteracting Hamiltonian of C when the coupling V is included. Eventually, self-energy terms accounting for the particle-particle interaction are included. As

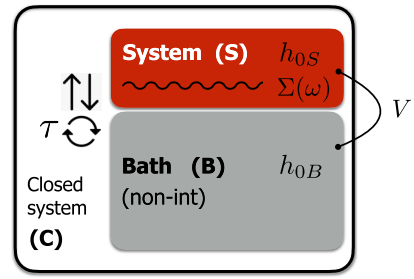

$$h_0, g_0 \qquad H_0, G_0 \qquad H, G$$

$$\begin{bmatrix} h_{0S} & 0 \\ 0 & h_{0B} \end{bmatrix} \quad \begin{bmatrix} h_{0S} & V \\ V^\dagger & h_{0B} \end{bmatrix} \quad \begin{bmatrix} h_{0S}+\Sigma & V \\ V^\dagger & h_{0B} \end{bmatrix}$$

FIG. 1. Top: Partitioning of the closed system C into the subparts S (interacting, as indicated by the wiggly line) and B (noninteracting). The Hamiltonian and self-energy blocks and the coupling V of the two subsystems are also indicated. Bottom: Sketch view of the three different Hamiltonians and Green's functions involved in the discussion of embedding. Left: S and B are noninteracting and uncoupled. Middle: S and B are noninteracting but coupled. Right: S is interacting and coupled to the noninteracting B.

discussed in Appendix A, since interactions are present only within S, one can show that the corresponding self-energy is limited to the same subsystem. Moreover, since h_{0B} is noninteracting, without loss of generality we may take it diagonal on the chosen basis, such that $h_{0B} = \mathrm{diag}(\Omega_1, \ldots, \Omega_n, \ldots)$.

Within the above definitions and following Fig. 1, we can define the Green's functions for the whole system C at different levels of description (noninteracting and uncoupled, noninteracting and coupled, interacting in S and coupled) according to

$$\begin{aligned} g_0(\omega) &= [\omega I - \mathrm{diag}(h_{0S}, h_{0B})]^{-1} = [\omega I - h_0]^{-1}, \\ G_0(\omega) &= [\omega I - H_0]^{-1}, \\ G(\omega) &= [\omega I - H_0 - \Sigma(\omega)]^{-1} \end{aligned} \tag{1}$$

(time-ordered offsets from the real axis are left implicit). We note that when G is the physical GF, then $\Sigma = \Sigma_{\mathrm{Hxc}}$ is the interaction self-energy (accounting for Hartree, exchange, and correlation terms). Nevertheless, in the following we will also consider cases where G is a trial GF, as discussed, e.g., in Sec. III B. In these cases, $\Sigma = \widetilde{\Sigma}$ just collects a set of degrees of freedom useful to represent G via the Dyson equation:

$$G = G_0 + G_0 \widetilde{\Sigma} G. \tag{2}$$

Within this construction, the self-energy $\widetilde{\Sigma}$ is also constrained to have nonzero matrix elements only within subsystem S (which can be seen as a domain definition for the set of trial G's).

By focusing on the subsystem S and making reference to the theory of Green's function embedding [5,13], the S blocks of the above GFs are obtained as

$$\begin{aligned} g_{0S}(\omega) &= [\omega I_S - h_{0S}]^{-1}, \\ G_{0S}(\omega) &= [\omega I_S - h_{0S} - \Delta v_S(\omega)]^{-1}, \\ G_S(\omega) &= [\omega I_S - h_{0S} - \Delta v_S(\omega) - \Sigma(\omega)]^{-1}, \end{aligned} \tag{3}$$

where Δv_S is an embedding self-energy due to the bath B [5,13,47,48,50]:

$$\Delta v_S(\omega) = V g_{0B}(\omega) V^\dagger = \sum_n \frac{R_n}{\omega - \Omega_n \pm i0^+}, \tag{4}$$

which acts as a correction to the external potential of S.

The total energy of the closed system C can be obtained variationally, e.g., via the Klein functional [20,22], reading

$$E^K[G] = \mathrm{Tr}_\omega \ln\{G_0^{-1} G\} + \mathrm{Tr}_\omega\{H_0 G_0\} + \mathrm{Tr}_\omega\{I - G_0^{-1} G\} + \Phi_{\mathrm{Hxc}}[G], \tag{5}$$

where we have defined $\mathrm{Tr}_\omega\{\cdots\} = \int \frac{d\omega}{2\pi i} e^{i\omega 0^+} \mathrm{Tr}\{\cdots\}$ and $\Phi_{\mathrm{Hxc}}[G]$ is a functional [19–21] to be approximated that is related to the interaction self-energy as

$$\frac{\delta \Phi_{\mathrm{Hxc}}[G]}{\delta G} = \frac{1}{2\pi i} \Sigma_{\mathrm{Hxc}}[G]. \tag{6}$$

With the above definitions, one can show [5,13] that the gradient of the Klein functional is zero for the GF G that satisfies the self-consistent Dyson equation

$$G = G_0 + G_0 \Sigma_{\mathrm{Hxc}}[G] G. \tag{7}$$

A. Sum over poles and algorithmic inversion

In the following, we make use of the concept of sum over poles (SOP) [27,28,31,51–53] to represent propagators, combined with the AIM [31,51,52] to solve Dyson-like equations. In practice, this amounts to writing propagators and self-energies using discrete poles and residues (meromorphic representations [27]) as

$$G_0(\omega) = \sum_n \frac{A_n^0}{\omega - \epsilon_n^0 \pm i0^+}, \tag{8}$$

$$G(\omega) = \sum_s \frac{A_s}{\omega - \epsilon_s \pm i0^+}, \tag{9}$$

$$\Sigma(\omega) = \Sigma_0 + \sum_n \frac{\Gamma_n}{\omega - \omega_n \pm i0^+}, \tag{10}$$

which could also be seen as discrete Lehmann representations [53]. This is physically meaningful before taking the thermodynamic limit and represents a mild assumption in dealing with propagators. Recently, SOPs were also used to represent the screened Coulomb interaction in the context of GW, leading to the multi-pole approximation (MPA) [56,57].

In Eqs. (8)–(10), G_0 is a noninteracting GF obtained from the single-particle Hamiltonian h_0,

$$h_0 |\phi_n^0\rangle = \epsilon_n^0 |\phi_n^0\rangle, \quad A_n^0 = |\phi_n^0\rangle\langle\phi_n^0|, \tag{11}$$

while G is an interacting or embedded GF, obtained from G_0 by a Dyson equation involving Σ, i.e., $G = [\omega I - h_0 - \Sigma(\omega)]^{-1}$. Conversely, if G and G_0 are given, the self-energy connecting them can be determined by inverting the Dyson equation as $\Sigma = G_0^{-1} - G^{-1}$. By assuming discrete and real poles for Σ and G_0, as well as Hermitian Σ_0 and positive semidefinite (PSD) residues Γ_n, we find [51,52,55] (see also Appendix A 1) that G also has real discrete poles and that its residues and poles satisfy

$$[h_0 + \Sigma(\epsilon_s)]|f_s\rangle = \epsilon_s |f_s\rangle, \quad A_s = |f_s\rangle\langle f_s|. \tag{12}$$

The normalization of $|f_s\rangle$ is given by [58]

$$\langle f_s | f_s \rangle = Z_s = 1 + \langle f_s | \dot{\Sigma}(\epsilon_s) | f_s \rangle \leqslant 1, \tag{13}$$

$$\sum_s |f_s\rangle\langle f_s| = I, \tag{14}$$

where $\dot{\Sigma}(\omega) = \partial\Sigma(\omega)/\partial\omega$. From Eq. (14), the $|f_s\rangle$ orbitals are complete, although not linearly independent or orthonormalized (see also Ref. [52]). In the expressions above, the Dyson equation is mapped to a nonlinear eigenvalue problem, Eq. (12), involving rational functions [51,52,55]. In passing we note that the positive semidefiniteness of the residues of G and Σ are closely related to each other when the two quantities are connected by a Dyson equation. In fact, given

$$A(\omega) = \frac{1}{2\pi i}[G(\omega) - G^\dagger(\omega)]\mathrm{sgn}(\mu - \omega),$$

$$\Gamma(\omega) = \frac{1}{2\pi i}[\Sigma(\omega) - \Sigma^\dagger(\omega)]\mathrm{sgn}(\mu - \omega), \tag{15}$$

$$A(\omega) = G(\omega)\Gamma(\omega)G^\dagger(\omega) \tag{16}$$

(the last identity comes from the Dyson equation), the positive semidefiniteness of A is equivalent [13,59] (i.e., if and only if) to that of Γ. In Appendix A 1 we provide a stronger result, valid for SOP propagators, connecting the well-behavedness of G to that of Σ.

Next, given G_0 and Σ represented as SOPs, it is possible to explicitly compute the coefficients of the Green's function G by solving the related Dyson equation. This can be achieved by mapping the nonlinear eigenvalue problem of Eq. (12) into a linear eigenproblem in a larger space. This approach, termed the algorithmic-inversion method (AIM), was introduced and detailed in Refs. [31,51,52]. Algebraically, the AIM-SOP method stems from identifying the interaction self-energy as an embedding self-energy [see Eqs. (28) and (29)] and then solving the Hamiltonian problem in the larger subspace. This is always possible within the conditions mentioned above (self-energy featuring real poles, Hermitian Σ_0, and positive semi-definite residues); see Appendix A 1 for a detailed discussion. Note, however, that the AIM-SOP technique is more general and can deal with self-energies not strictly fulfilling all requirements, according to Appendix A 1, of physical embedding (details are provided in Refs. [51,52]). We also note that similar techniques have been used in the context of dynamical mean-field theory [60–62], lattice Hamiltonians [27], and, more recently, GW and the Bethe-Salpeter equation formalism [63,64].

III. ANALYTICAL EVALUATION OF Trln TERMS

As a technical prerequisite for this work and as a relevant result in itself, in this section we focus on integrals of the form

$$\Delta E_K = \mathrm{Tr}_\omega \ln\{G_0^{-1} G\} = \int \frac{d\omega}{2\pi i} e^{i\omega 0^+} \mathrm{Trln}\{G_0^{-1}(\omega) G(\omega)\}. \tag{17}$$

By representing the Green's functions G_0 and G in the above equation as SOPs according to Eqs. (8) and (9), we can derive a general analytical expression for ΔE_K of Eq. (17), as shown below. In order to do this, we make use of some common

operator and matrix identities, which we report here for completeness. For instance, we use the following identity:

$$\mathrm{Trln}(A) = \ln\det(A). \tag{18}$$

Bearing Eq. (18) in mind, by using the identity $\det(AB) = \det(A)\det(B)$, the following relation also holds:

$$\mathrm{Trln}(AB) = \mathrm{Trln}(A) + \mathrm{Trln}(B). \tag{19}$$

Moreover, given a matrix A represented in the block form

$$A = \begin{bmatrix} S & V_1 \\ V_2^\dagger & B \end{bmatrix}, \tag{20}$$

if B is invertible, the determinant of A can be expressed as [65]

$$\det(A) = \det(B)\det(S - V_1 B^{-1} V_2^\dagger), \tag{21}$$

which is a result reminiscent of techniques used in GF embedding, presented in Sec. II.

A. Special case: Noninteracting *G*

As a first step, we consider the case where both G_0 and G in Eq. (17) are noninteracting GFs corresponding to mean-field Hamiltonians h_0 and h_1, defined as

$$h_i = \sum_m |\phi_m^i\rangle \epsilon_m^i \langle\phi_m^i|. \tag{22}$$

This means that both G_0 and G are diagonal on single-particle orthonormal basis sets ($|\phi_m^0\rangle$ and $|\phi_m^1\rangle$), which can be used to evaluate the traces. Importantly, we assume that the number of occupied electrons is the same for G_0 and G. By considering Eq. (19) and taking $A = G_0^{-1}$ and $B = G$, we can write the ΔE_K integral as

$$\Delta E_K = \int \frac{d\omega}{2\pi i} e^{i\omega 0^+} [-\mathrm{Trln}G_0 + \mathrm{Trln}G], \tag{23}$$

$$= \int \frac{d\omega}{2\pi i} e^{i\omega 0^+} \left[\ln \frac{\Pi_m^{\mathrm{all}}(\omega - \epsilon_m^0 \pm i0^+)}{\Pi_m^{\mathrm{all}}(\omega - \epsilon_m^1 \pm i0^+)}\right]. \tag{24}$$

The label "all" in the product means that both occupied and empty poles are considered. In order to evaluate the integral using residues, the contour needs to be closed in the upper half plane, the enclosed poles corresponding to occupied states of both G_0 and G. Since the number of occupied poles of both systems is the same, the integral ΔE_K can be rewritten as

$$\Delta E_K = \sum_m^{\mathrm{occ}} \oint_{\Gamma_m} \frac{dz}{2\pi i} \ln \frac{z - \epsilon_m^0 - i0^+}{z - \epsilon_m^1 - i0^+}, \tag{25}$$

with an example of a Γ_m contour represented in Fig. 3 in Appendix B 1. The analytical expression for contour integrals such as those appearing in Eq. (25) is provided in Eq. (B1). Taking advantage of that expression, we recover the well-known result [5,13,25,36]

$$\Delta E_K = \sum_m^{\mathrm{occ}} \left[n_m^1 \epsilon_m^1 - n_m^0 \epsilon_m^0\right], \tag{26}$$

where we have made the eigenvalue multiplicities n_m^i explicit and limited the sum to distinct multiplets.

B. General case: Interacting *G*

Next, in this section we consider the case of Eq. (17) with a fully interacting G. Without loss of generality, we can define a self-energy connecting G and G_0 by a Dyson equation by writing

$$\Sigma(\omega) = G_0^{-1} - G^{-1}. \tag{27}$$

It is important to note that such self-energy is not necessarily physical (i.e., it may not originate from perturbation theory or from a functional formulation), but rather an auxiliary mathematical object. Since G_0, G, and Σ are connected by a Dyson equation and with the assumption of discrete poles for both G_0 and G (which then result in meromorphic functions of the frequency), Σ also has discrete poles. We are therefore in the position to use the SOP representations given in Eqs. (8)–(10). In what follows we represent single-particle operators on a truncated basis set, thereby mapping them to finite-dimensional matrices.

According to the definitions and results in Appendix. A 1 and to the discussion in Sec. II A, G being well-behaved (real poles, positive semidefinite and complete residues) implies that Σ is also well-behaved (real poles, positive semidefinite residues, Hermitian asymptotic value). Therefore, since the residues Γ_n of Σ are PSD, following Refs. [31,51,52], we can introduce V_n such that

$$\Gamma_n = V_n V_n^\dagger. \tag{28}$$

In doing so, V_n can be taken, e.g., to be the square root of Γ_n or to be a lower-rank rectangular matrix (when represented on a basis) if Γ_n is low rank. As a result, G can be seen as the GF of an embedded system (index 0, below) coupled to an external bath. Indeed, by defining the inverse resolvent $(\omega I - \mathcal{H})$ of the whole auxiliary system as

$$\omega I - \mathcal{H} = \begin{bmatrix} \omega I - h_0 & V_1 & V_2 & \dots \\ V_1^\dagger & (\omega - \omega_1)I & & \\ V_2^\dagger & & (\omega - \omega_2)I & \\ \vdots & & & \ddots \end{bmatrix},$$

$$= \begin{bmatrix} S & V \\ V^\dagger & B \end{bmatrix}, \tag{29}$$

we can immediately verify that the self-energy in Eq. (10) is the embedding self-energy for the zeroth-block subsystem S (in the following, calligraphic operators such as $\mathcal{H}$ refer to the enlarged auxiliary space). This construction is the same as that used in the framework of the algorithmic-inversion method [31,51], used to solve Dyson equations involving propagators represented as SOP, and presented in Sec. II A. As discussed in Appendix A 2, if the input G is well-behaved, the above embedding construction is always possible and leads to a Hermitian Hamiltonian $\mathcal{H}$. Overall, with $\mathcal{H}$ being noninteracting, Theorem 1 in Appendix A 1 *de facto* provides a dynamical (in the embedding sense presented above) *noninteracting v-representability* condition for G (in the embedding sense presented above), which is a general and relevant result per se.

We can now apply the identity in Eq. (21) to the matrix in Eq. (29), obtaining

$$\det(\omega I - \mathcal{H}) = \det(B)\det(S - VB^{-1}V^\dagger)$$

$$= \prod_n (\omega - \omega_n)^{r_n} \det(\omega I - h_0 - \Sigma), \tag{30}$$

where r_n is the rank of the Γ_n matrix. The above equation can be recast in the following form:

$$\det G(\omega) = \prod_n (\omega - \omega_n)^{r_n} \det(\omega I - \mathcal{H})^{-1} \tag{31}$$

$$= \frac{\prod_n^{\text{all}} (\omega - \omega_n)^{r_n}}{\prod_s^{\text{all}} (\omega - \epsilon_s)^{n_s}}, \tag{32}$$

where we have exploited the fact that the poles of G are also eigenvalues of $\mathcal{H}$ for the whole system and made the multiplicities n_s explicit.

Combining Eq. (23) with Eq. (18), we obtain

$$\Delta E_K = \int \frac{d\omega}{2\pi i} e^{i\omega 0^+} [\ln \det G - \ln \det G_0],$$

$$= \int \frac{d\omega}{2\pi i} e^{i\omega 0^+} \ln \left[\frac{\prod_n^{\text{all}} (\omega - \omega_n)^{r_n} \prod_m^{\text{all}} \left(\omega - \epsilon_m^0\right)^{n_m^0}}{\prod_s^{\text{all}} (\omega - \epsilon_s)^{n_s}} \right]. \tag{33}$$

$$= \int \frac{d\omega}{2\pi i} e^{i\omega 0^+} \, \text{Trln}\left\{\mathcal{G}_0^{-1}(\omega)\mathcal{G}(\omega)\right\}. \tag{34}$$

In the last equation, $\mathcal{G}$ and $\mathcal{G}_0$ are the GFs of the auxiliary system obtained with and without including the coupling matrices V in $\mathcal{H}$, respectively. A counting of the degrees of freedom shows that the cardinality of $\{\epsilon_s\}$ is equal to that of $\{\epsilon_m^0\} \cup \{\omega_n\}$, as also shown by the embedding construction in Eq. (29). Nevertheless, only occupied poles (i.e., poles above the real axis) count in the integral.

If the numbers of such poles in the numerator and in the denominator are the same, by exploiting Eq. (25) we obtain the final result:

$$\Delta E_K = \sum_s^{\text{occ}} n_s \epsilon_s - \left[\sum_m^{\text{occ}} n_m^0 \epsilon_m^0 + \sum_n^{\text{occ}} r_n \omega_n \right]. \tag{35}$$

This expression is the first key result of the present work. The condition of having the same number of occupied states in the numerator and denominator in the second line of Eq. (33) is equivalent to having the same number of occupied states before and after the introduction of the coupling matrix elements V. This condition, therefore, encodes charge conservation within the closed system $C = S \cup B$. In Appendix B 3 we also provide a generalization of Eq. (35) in which both propagators in the Trln term are interacting (or embedded).

At this point it is worth discussing alternative approaches in the literature aimed at evaluating terms of the form $\text{Tr}_\omega \ln\{G_0^{-1} G_1\}$. For instance, in a series of papers, Dahlen and coworkers [24–26] first rewrote the Trln term of the Luttinger-Ward functional by factorizing the static part of the self-energy Σ_x and then recasting [26] the integral for numerical integration over the imaginary axis. Along the same lines, in Appendix B 2 we provide a scheme for numerical integration of the Trln terms that we use in the present work to numerically validate analytical expressions such as Eq. (35). In Ref. [27], Friesen and coworkers (who also adopted a meromorphic, i.e., SOP in our terminology, representation for the propagators) first handled the Σ_x term as in Refs. [24–26] and then numerically evaluated the residual contribution to the integral using a coupling-constant integration. In Ref. [36], Ismail-Beigi discussed the RPA correlation energy in the context of Green's function theory and, exploiting algebraic techniques similar to those employed in this work, provided an analytical expression involving the poles of the independent-particle and RPA response functions. We discuss the RPA correlation energy in Sec. IV A, where we rederive Ismail-Beigi's expression by means of the present formalism. Additionally, Aryasetiawan *et al.* [66] wrote the RPA correlation energy in a form similar to that of Ref. [26] and Appendix B 2 for numerical evaluation along the imaginary axis.

IV. APPLICATIONS

Having derived an analytical expression for the Trln terms defined by Eq. (17), a result already relevant per se (notably allowing one to easily evaluate the Klein functional within the SOP formulation), in this section we present two further applications of Eq. (35). First, we focus on the calculation of the RPA correlation energy, providing a rederivation of a result already known in the literature [36], and then we apply the formalism to analyze and partition the Klein functional in the presence of embedding.

A. RPA correlation energy

In the context of Green's function methods, the RPA correlation energy (Fig. 2) is written as [5,13,18,22,36–39]

$$P(\mathbf{x}_1, \mathbf{x}_2, \omega) = \int \frac{d\omega'}{2\pi i} G(\mathbf{x}_1, \mathbf{x}_2, \omega + \omega') G(\mathbf{x}_2, \mathbf{x}_1, \omega'),$$

$$\Phi_c^{\text{RPA}}[P] = -\frac{1}{2}\text{Tr}_\omega \left\{ \sum_{n=2}^{\infty} \frac{1}{n} [vP(\omega)]^n \right\} \tag{36}$$

$$= +\frac{1}{2}\text{Tr}_\omega \ln\{I - vP(\omega)\} + \frac{1}{2}\text{Tr}_\omega\{vP\}$$

$$= \Delta\Phi_1^{\text{RPA}} + \Delta\Phi_2^{\text{RPA}}, \tag{37}$$

where the irreducible polarizability P can be evaluated e.g. using the Kohn-Sham Green's function G_s as in the optimized-effective-potential method [32] or by an interacting Green's function (e.g., at the level of self-consistent GW, when making the Klein or Luttinger-Ward functional stationary [5,13,19–21]). By considering the Dyson equation

$$\chi(\omega) = P(\omega) + \chi(\omega) v P(\omega), \tag{38}$$

connecting the irreducible and reducible polarizabilities (P and χ, respectively), we obtain

$$I - vP = \epsilon = \chi^{-1} P, \tag{39}$$

which can be used in the first term, $\Delta\Phi_1^{\text{RPA}}$, of Eq. (37), leading to

$$\Phi_c^{\text{RPA}}[P] = -\tfrac{1}{2}\text{Tr}_\omega \ln\{P^{-1}\chi\} + \tfrac{1}{2}\text{Tr}_\omega\{vP\}. \tag{40}$$

By considering χ and P to be two interacting single-particle propagators, we can apply Eqs. (B10) and (B11) with $\Sigma_{21} = v$ in view of Eq. (38). This means that the poles of the two self-energies need to cancel out identically and therefore do not

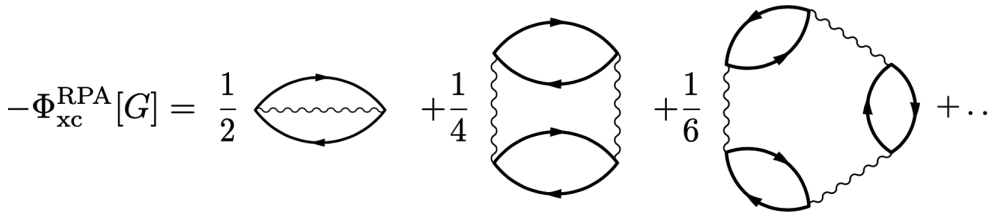

FIG. 2. Exchange (first term) plus RPA correlation energy represented by means of Feynman diagrams.

contribute to the evaluation of the Trln term. In turn, we obtain

$$\Delta\Phi_1^{\mathrm{RPA}} = -\frac{1}{2}\sum_p^{\Omega_p^{(0)}<0}\left[n_p\Omega_p - n_p^0\Omega_p^0\right] = \frac{1}{2}\sum_p^{\Omega_p^{(0)}>0}\left[n_p\Omega_p - n_p^0\Omega_p^0\right], \tag{41}$$

where Ω_p and Ω_p^0 are the poles of χ and P, respectively, and we have considered that each time-ordered polarizability has poles at $\pm|\Omega_p^{(0)}|$, with the negative ones being those above the real axis and contributing to the integral. Degeneracies of the poles (n_p and n_p^0) have been marked explicitly.

We now turn to the evaluation of the second term, $\Delta\Phi_2^{\mathrm{RPA}}$, in Eq. (37). The irreducible polarizability P can be represented as a sum over poles according to

$$P(\omega) = \sum_p^{\Omega_p^0>0}\left[\frac{|t_p\rangle\langle t_p|}{\omega-\Omega_p^0+i0^+} - \frac{|t_p\rangle\langle t_p|}{\omega+\Omega_p^0-i0^+}\right], \tag{42}$$

where $\langle\mathbf{x}|t\rangle = \phi_c(\mathbf{x})\phi_v^*(\mathbf{x})$, with c and v referring to conduction and valence single-particle orbitals, respectively. With the above definitions, we obtain

$$\Delta\Phi_2^{\mathrm{RPA}} = -\frac{1}{2}\sum_p^{\Omega_p^0>0}\langle t_p|v|t_p\rangle, \tag{43}$$

which completes the evaluation of the RPA correlation energy, consistent with the existing literature. In particular, we have recovered Eq. (23) of Ref. [36].

B. Embedding of the Klein functional

The main goal of the present section is to study the Klein functional in the presence of an embedding scheme such as the one described in Sec. II and Appendix A in order to derive, as demonstrated below, a variational partition of the total energy. In order to do so we begin by partitioning each term appearing in the Klein functional given by Eq. (5). Notably, the functional depends on a trial Green's function G that, according to Eq. (2), we represent by means of a self-energy $\widetilde{\Sigma}$ constrained to be localized on the subsystem S. As discussed in Sec. II, this represents a definition of the domain of the trial GF G.

With regard to Φ_{Hxc}, the partition is already in place since the particle-particle interaction is present only in S. Therefore, we have

$$\Phi_{\mathrm{Hxc}}[G] = \Phi_{\mathrm{Hxc}}[G_S]. \tag{44}$$

This can be understood, e.g., diagrammatically since the bare interaction lines connect only points in the S subsystem, causing each vertex to be located in S. This is further discussed in Appendix A. Next, we consider the $\mathrm{Tr}_\omega H_0 G_0$ term, which is the noninteracting energy of the closed $C = S\cup B$ system and can be partitioned as

$$\mathrm{Tr}_\omega\{H_0G_0\} = \mathrm{Tr}_\omega^S\{(h_{0S}+\Delta v_S)G_{0S}\} + \mathrm{Tr}_\omega^B\{(h_{0B}+\Delta v_B)G_{0B}\} \tag{45}$$

$$= \sum_s^{\mathrm{occ}}\epsilon_s^0, \tag{46}$$

where ϵ_s^0 are the eigenvalues of the noninteracting problem for C, $H_0|\phi_s\rangle = \epsilon_s^0|\phi_s\rangle$.

Coming to the next term, the following chain of identities also holds:

$$\begin{aligned}\mathrm{Tr}_\omega\left\{I - G_0^{-1}G\right\} &= -\mathrm{Tr}_\omega\{\widetilde{\Sigma}G\}\\ &= -\mathrm{Tr}_\omega^S\{\widetilde{\Sigma}_S G_S\}\\ &= \mathrm{Tr}_\omega^S\left\{I_S - G_{0S}^{-1}G_S\right\},\end{aligned} \tag{47}$$

where we have represented the trial G according to Eq. (2) and limited $\widetilde{\Sigma}$ to have nonzero matrix elements only in S and to have a regular propagatorlike analytical structure featuring time-ordering and simple (first-order) poles. Indeed, the last step is valid because of the following equation:

$$G_S = G_{0S} + G_{0S}\widetilde{\Sigma}_S G_S. \tag{48}$$

Finally, the first term in Eq. (5), $\mathrm{Tr}_\omega \ln G_0^{-1}G$, can be evaluated using Eq. (35):

$$\begin{aligned}\mathrm{Tr}_\omega\ln\left\{G_0^{-1}G\right\} &= \sum_s^{\mathrm{occ}}\epsilon_s - \sum_n^{\mathrm{occ}}\epsilon_n^0 - \sum_n^{\mathrm{occ}}\mathrm{poles}(\widetilde{\Sigma})\\ &= \mathrm{Tr}_\omega^S\ln\left\{G_{0S}^{-1}G_S\right\},\end{aligned} \tag{49}$$

where we have used the fact that $\sum_s\epsilon_s = \sum\mathrm{poles}(G_S)$ and $\sum_n\epsilon_n^0 = \sum\mathrm{poles}(G_{0S})$. Using the notation introduced in Eqs. (3) and (4), where Ω_n are the poles of the embedding self-energy, we can show that the term $\sum_n\Omega_n = \sum\mathrm{poles}(\Delta v_S)$ does not explicitly appear because the embedding self-energy is used in the evaluation of both the G_{0S} and G_S Green's functions. Multiplicities have been kept implicit in the sums over eigenvalues.

Alternatively, the same result can be obtained directly from the use of Eq. (18) and the identity concerning the determinant of block matrices, Eq. (21). In particular, from

$$G^{-1}(\omega) = \begin{bmatrix}\omega I_S - h_{0S} - \widetilde{\Sigma} & -V\\ -V^\dagger & \omega I_B - h_{0B}\end{bmatrix}, \tag{50}$$

we get

$$\det G^{-1} = \det g_{0B}^{-1} \det G_S^{-1}, \tag{51}$$

$$\det G_0^{-1} = \det g_{0B}^{-1} \det G_{0S}^{-1}, \tag{52}$$

which give

$$\begin{aligned} \mathrm{Tr}_\omega \ln\{G_0^{-1} G\} &= -\ln\det g_{0B}^{-1} - \ln\det G_S^{-1} \\ &\quad + \ln\det g_{0B}^{-1} + \ln\det G_{0S}^{-1} \\ &= \ln\det G_{0S}^{-1} G_S; \end{aligned} \tag{53}$$

The last line is equivalent to the result to be proven.

We are now in the position to put all terms together to obtain

$$\begin{aligned} E_K[G] &= \mathrm{Tr}_\omega^S \ln\{G_S G_{0S}^{-1}\} + \sum_s^{\mathrm{occ}} \epsilon_s^0 \\ &\quad + \mathrm{Tr}_\omega^S\{I_S - G_{0S}^{-1} G_S\} + \Phi_{\mathrm{Hxc}}[G_S]. \end{aligned} \tag{54}$$

Next, the first term on the right-hand side can be further rewritten using

$$\begin{aligned} \mathrm{Tr}_\omega^S \ln\{G_S G_{0S}^{-1}\} &= \mathrm{Tr}_\omega^S \ln\{G_S g_{0S}^{-1}\, g_{0S} G_{0S}^{-1}\} \\ &= \mathrm{Tr}_\omega^S \ln\{G_S g_{0S}^{-1}\} \\ &\quad - \mathrm{Tr}_\omega^S \ln\{G_{0S} g_{0S}^{-1}\}, \end{aligned} \tag{55}$$

$$\mathrm{Tr}_\omega^S \ln\{G_{0S} g_{0S}^{-1}\} = \sum_s^{\mathrm{occ}} \epsilon_s^0 - \sum_s^{\mathrm{occ}} \bar{\epsilon}_s^0 - \sum_n^{\mathrm{occ}} \Omega_n \tag{56}$$

$$\begin{aligned} &= \sum_s^{\mathrm{occ}} \epsilon_s^0 - \mathrm{Tr}_\omega^S\{h_{0S} g_{0S}\} \\ &\quad - \mathrm{Tr}_\omega^B\{h_{0B} g_{0B}\} \end{aligned} \tag{57}$$

where the eigenvalues $\bar{\epsilon}_s^0$ refer to subsystem S in the absence of coupling to B.

Eventually, this leads to the final result for the partitioning of the Klein energy functional:

$$E_K[G] = E_K^S[G_S] + \mathrm{Tr}_\omega^B\{h_{0B} g_{0B}\}, \tag{58}$$

$$\begin{aligned} E_K^S[G_S] &= \mathrm{Tr}_\omega^S \ln\{G_S g_{0S}^{-1}\} + \mathrm{Tr}_\omega^S\{h_{0S} g_{0S}\} \\ &\quad + \mathrm{Tr}_\omega^S\{I_S - g_{0S}^{-1} G_S\} + \mathrm{Tr}_\omega^S\{\Delta v_S G_S\} + \Phi_{\mathrm{Hxc}}[G_S]. \end{aligned} \tag{59}$$

This is the second key result of the present paper, implying that $E_K^S[G_S]$ is stationary for the G_S that solve the embedding Dyson equation, namely,

$$2\pi i \frac{\delta E_K^S[G_S]}{\delta G_S} = G_S^{-1} - g_{0S}^{-1} + \Delta v_S + \Sigma_{\mathrm{Hxc}}[G_S] = 0, \tag{60}$$

showing that the partition of the Klein energy is exact and also variational with respect to subsystem S.

Interestingly, we note that an equation formally equivalent to Eq. (59) was used by Savrasov and Kotliar [40,67] to express the grand potential of a quantum system in the presence of an external local and dynamical potential coupled to the local Green's function. In the present context, that term is played by Δv_S, here originating from an embedding procedure. Interestingly, the embedding construction allows us to further inspect the physical nature of the energy terms in Eqs. (58) and (59). In particular, the complement energy $\mathrm{Tr}_\omega^B\{h_{0B} g_{0B}\}$ (i.e., the energy that needs to be summed to $E_K^S[G_S]$ to give the total energy of the closed system C, $E_K[G]$) is that of the noninteracting and uncoupled bath. This means that all effects of the coupling V need to be absorbed in $E_K^S[G_S]$ to allow for variationality. This is at variance with other possible partitions of the C total energy (such as those suggested by the Galitskii-Migdal expression).

V. CONCLUSIONS

In this work, within the framework of Green's function methods, we addressed the use of the Klein functional when embedding an interacting system S into a noninteracting bath B. Exploiting a meromorphic (sum-over-poles) representation for the propagators and taking advantage of the algorithmic inversion method introduced to solve Dyson-like equations involving SOP propagators [31,51,52], we first derived an exact analytical expression to evaluate terms of the form $\mathrm{Tr}_\omega \ln\{G_0^{-1} G\}$. Notably, such terms appear in the Klein and Luttinger-Ward functionals [5,13,19–21] as well as in other common many-body terms such as the RPA correlation energy [5,13,18,22,36–39]. In this respect, the analytical expression obtained represents the first key result of the present paper.

Next, we used the above analytical result to partition the Klein functional of an embedded system into two contributions, one associated with the subsystem S and one associated with the noninteracting bath B. Importantly, the energy associated with S is also variational as a functional of the S Green's function G_S, with the functional gradient becoming zero for the physical embedded G_s. This is the second main result of the work. Last, we also exploited the analytical result for the Trln terms to recover an exact analytical expression for the RPA correlation energy known in the literature [36].

In perspective, the analytical expression obtained for the Trln term, Eq. (35), complements the set of analytical results stemming from the use of the SOP representation of propagators, notably including the algorithmic-inversion method (which is further developed in Appendix A 1 to compute G^{-1}, together with the definition of a dynamical noninteracting v-representability condition for G.) In turn, the SOP formulation has the potential to further support the use of dynamical approaches (i.e., exploiting dynamical potentials, possibly made variational using the Klein or Luttinger-Ward functional, now written explicitly in terms of poles and residues of the GF) in electronic-structure theory and calculations. An example of such a formulation can be found in Refs. [51,52]. Moreover, the exact embedding partition obtained for the Klein functional allows for a variational formulation of the embedding process and for a better physical understanding of the whole formulation. In turn, this may be relevant to a number of theoretical frameworks exploiting embedding techniques.

ACKNOWLEDGMENTS

We thank Prof. M. Gibertini and Prof. L. Reining for useful discussions on the subject. We also thank M. Quinzi for reading the manuscript and for providing further numerical validation for some of the analytical results presented. This

work was supported by the Swiss National Science Foundation (SNSF) through Grant No. 200020-213082 (T.C.) and NCCR MARVEL (N.M.), a National Centre of Competence in Research through Grant No. 205602.

APPENDIX A: COMPLEMENTARY DETAILS OF GREEN'S FUNCTION EMBEDDING

1. Well-behavedness of SOP propagators

In this section we discuss the conditions to be fulfilled in order to obtain propagators that are well-behaved. We do this for propagators expressed in SOP form by introducing the following definitions.

Definition 1. A Green's function G in SOP form according to Eq. (9) is said to be *well-behaved (wb)* if it has real poles and Hermitian and positive semidefinite residues, which also satisfy the completeness relation $\sum_s A_s = I$.

Definition 2. Similarly, a self-energy Σ in the form of Eq. (10) is said to be *well-behaved (wb)* if it has real poles, Hermitian and positive semidefinite residues, and a Hermitian asymptotic limit Σ_0.

As an example, noninteracting Green's functions are well-behaved, and the property remains valid also when the GF is projected on a subspace of the initial domain. Choosing a reference noninteracting $G_0(z) = [zI - h_0]^{-1}$ and considering all propagators expressed in SOP form with discrete poles, it is then possible to make the following statement.

Theorem 1. Given G and Σ connected by a Dyson equation $G = G_0 + G_0\Sigma G$, G is well-behaved if and only if Σ is well-behaved.

Proof. The implication $\Sigma\ wb \Rightarrow\ G\ wb$ can be immediately demonstrated by using the AIM-SOP technique according to Eqs. (28) and (29), where an auxiliary noninteracting Hamiltonian $\mathcal{H}$ in a larger space is devised and used to build the Green's function G. As also discussed in Refs. [31,51,52], when Σ is *wb*, the Hamiltonian $\mathcal{H}$ becomes Hermitian, which implies the thesis. Next, we focus on the inverse implication, $G\ wb \Rightarrow\ \Sigma\ wb$. By inverting the Dyson equation we have $\Sigma(z) = G_0(z) - G^{-1}(z)$, so we aim at building a variant of the AIM-SOP technique to compute G^{-1}. In order to do so, we write

$$\begin{aligned} \Sigma(z) &= zI - h_0 - (z^2 - \Omega^2)F(z), \\ F(z) &= [(z^2 - \Omega^2)G(z)]^{-1}, \end{aligned} \tag{A1}$$

where Ω is chosen such that $\Omega^2 > \max(\epsilon_s^2, |\Omega_m|^2)$, where ϵ_s and Ω_m are the poles and zeros of G [68], respectively, here assumed to be bound. We note that the introduction of the Ω term, while not strictly needed, is done for convenience and the final result does not depend on it. With the above definitions we have

$$F^{-1}(z) = zI - \sum_s(-\epsilon_s A_s) - \sum_s \frac{A_s}{z - \epsilon_s}\left(\Omega^2 - \epsilon_s^2\right). \tag{A2}$$

Since ϵ_s are real by hypothesis, the second term on the right-hand side is Hermitian, and the residues of the poles in the third term are positive semidefinite (besides the global minus sign); the last two terms can be thought of as a *wb* self-energy, so the propagator $F(z)$ is also *wb* and can be written as

$$F(z) = \sum_m \frac{B_m}{z - \Omega_m} + \frac{B^+}{z - \Omega} + \frac{B^-}{z + \Omega}. \tag{A3}$$

In writing the above expression we have made use of the fact that, according to Eq. (A1), $\pm\Omega$ are, by construction, poles of F and its remaining poles are the zeros of G. As stated, we also have $\Omega^2 > \Omega_m^2$. Next, we use Eq. (A1) to evaluate the self-energy and compute

$$\begin{aligned} (z^2 - \Omega^2)F(z) = zI + \left[\sum_m \Omega_m B_m + \Omega B^+ - \Omega B^-\right] \\ + \sum_m \frac{B_m}{z - \Omega_m}\left(\Omega_m^2 - \Omega^2\right). \end{aligned} \tag{A4}$$

The expression above has a Hermitian constant term and negative semidefinite residues, which used together with Eq. (A1) show that Σ is well-behaved. This completes the proof. ■

In passing, we note that the modified AIM-SOP for G^{-1} presented above is relevant per se and further complements the list of operations that can be performed within the SOP formalism.

2. Feasibility of the embedding construction for G

In this section we discuss the conditions to be fulfilled in order to establish the embedding construction of Sec. III B once an input G is provided. Building on the results in the previous section, we can follow the logical steps in the formulation of the embedding construction. (1) Given G and choosing a reference noninteracting G_0, we can always compute a self-energy connecting the two propagators as $\Sigma(\omega) = G_0^{-1} - G^{-1}$. (2) Within the overall hypothesis of discrete poles and states, if G is well-behaved, the self-energy is also well-behaved (see Theorem 1 in Appendix A 1). (3) In turn, this allows one to build the embedding construction involving the closed system $C = S \cup B$ according to Eqs. (28) and (29), with an overall Hamiltonian matrix that is Hermitian (resulting from the self-energy poles being real and the residues being positive definite). (4) As discussed in Refs. [31,51,52], the embedding construction can also be made under more general conditions (complex poles, non-Hermitian residues), leading, in general, to non-Hermitian Hamiltonians for system C. Overall, the formal result in Appendix A 1 and the discussion above provide noninteracting v-representability conditions for a given Green's function G. Indeed, a well-behaved G can always be obtained from the embedding of a noninteracting system.

3. Green's function embedding and perturbation theory

In this section we discuss the formulation of many-body perturbation theory to include particle interaction effects in the Green's function in the presence of embedding. We consider the case of fermions at $T = 0$ for simplicity. As mentioned in Sec. II and sketched in Fig. 1, we consider a closed quantum system C partitioned into two subunits, $C = S \cup B$, interacting via a coupling potential V, with particle interactions confined to the S region, with B being a noninteracting bath. The particle-particle interaction V_{ee} (not to be confused

with the one-body coupling V) can be written in the usual form of a two-body potential:

$$V_{ee} = \frac{1}{2}\int d\mathbf{x}d\mathbf{x}'\,\hat{\psi}^\dagger(\mathbf{x})\hat{\psi}^\dagger(\mathbf{x}')\,v_{\rm int}(\mathbf{x},\mathbf{x}')\,\hat{\psi}(\mathbf{x}')\hat{\psi}(\mathbf{x}),$$
$$v_{\rm int}(\mathbf{x},\mathbf{x}') \neq 0 \quad \mathbf{x},\mathbf{x}' \in S, \tag{A5}$$

where the constraint on $v_{\rm int}(\mathbf{x},\mathbf{x}')$ expresses the fact that the interaction is present only in the S region.

Within the above definitions, the perturbation expansion for the Green's function of the closed system C leads to [5,13,18]

$$iG(\mathbf{x},t;\mathbf{x}',t') = \sum_{n=0}^{\infty}\frac{(-i)^n}{n!}\int_{-\infty}^{+\infty}dt_1\cdots dt_n \times \frac{\langle\Phi_0|\mathcal{T}[\hat{V}_{ee}(t_1)\cdots\hat{V}_{ee}(t_n)\,\hat{\psi}(\mathbf{x},t)\hat{\psi}^\dagger(\mathbf{x}',t')]|\Phi_0\rangle}{\langle\Phi_0|\hat{S}|\Phi_0\rangle}, \tag{A6}$$

$$\langle\Phi_0|\hat{S}|\Phi_0\rangle = \sum_{n=0}^{\infty}\frac{(-i)^n}{n!}\int_{-\infty}^{+\infty}dt_1\cdots dt_n \times \langle\Phi_0|\mathcal{T}[\hat{V}_{ee}(t_1)\cdots\hat{V}_{ee}(t_n)\,]|\Phi_0\rangle. \tag{A7}$$

First, we focus on G_S, i.e., on the case when $\mathbf{x}$ and $\mathbf{x}'$ are located in S. Since $\hat{V}_{ee}$ contains only field operators related to subspace S, all self-energy diagrams resulting from Eq. (A6) have only vertexes within subsystem S. Similarly, if we consider G in the general case (end points in either B or S), B points will be present only in disconnected diagrams (to be dropped) or at the external ends of the connected diagrams, which do not show in the proper self-energy. Therefore, the interaction self-energy is zero for matrix elements out of the S block, as shown in Fig. 1.

So far, perturbation theory in terms of the bare Green's function G_0 has been addressed, with $\Sigma_S[G_0] = \Sigma_S[G_{0S}]$. Nevertheless, we can perform the usual steps [5,13,18] in passing from bare diagrams involving G_0 to skeleton diagrams involving G, leading to

$$\Sigma_S[G] = \Sigma_S[G_S], \tag{A8}$$

where we can substitute G_S with G because of the localization of the bare interaction, Eq. (A5). A similar reasoning can be applied to the Φ functional to obtain $\Phi_{\rm Hxc}[G] = \Phi_{\rm Hxc}[G_S]$. In summary, within the noninteracting bath condition, the interaction self-energy Σ_S has a perturbation expansion structurally identical to the one usually developed for closed systems [5,13,18] and does not make any reference to the B unit; i.e., all diagrams develop within S, as if S were disconnected from B. Of course, G_S is then calculated in the presence of the bath, i.e., including embedding self-energies. Notably, the Anderson impurity model [5,40,69] can be seen as a special case of the above setting. Indeed, the exact electron-electron self-energy of the model is localized on the impurity [69] (S in our notation) and can be computed, e.g., using bare perturbation theory [40,70–72] involving G_{0S}.

As a relevant point for the present discussion, the use of the skeleton perturbation theory and the Luttinger-Ward functional was recently questioned [73–78], leading to a discussion about the domain of the trial G and the rise of multiple solutions of the nonlinear Dyson equation involving $\Sigma[G]$ (see, e.g., Ref. [78] for additional details). For the sake of the present work, we assume we are in the situation where perturbation theory does not pose convergence problems and one is able to discriminate between physical and unphysical solutions when needed.

APPENDIX B: COMPLEMENTARY DETAILS ON THE TrLn TERMS

1. Notable integrals

In this section we provide a detailed derivation of the expression

$$I = \oint_\Gamma \frac{dz}{2\pi i}\ln\frac{z-a}{z-b} = b-a, \tag{B1}$$

where both a and b are assumed to be real numbers. Making reference to Fig. 3, the contour integral can be split into four contributions, labeled Γ_1–Γ_4, such that $I = I_1 + I_2 + I_3 + I_4$, with $I_i = \int_{\Gamma_i}[\cdots]$.

Let us first consider I_1, where we assume that Γ_1 corresponds to the pole in a. Using the parametrization $z = Re^{i\theta}$, we have

$$I_1 = \int_{\Gamma_1}\frac{dz}{2\pi i}\ln\frac{z-a}{z-b} = -R\int_0^{2\pi}\frac{d\theta}{2\pi}e^{i\theta}\ln\left[1+\frac{a-b}{Re^{i\theta}}\right], \tag{B2}$$

which goes to zero in the limit $R\to 0$, e.g., in view of $R\ln(1/R)\to 0$. A similar argument holds for I_3, so that we have $I_{1,3}\to 0$ when $R\to 0$. Coming to the remaining paths, we have

$$I_{2+4} = \frac{1}{2\pi i}\left[-\int_{a+R}^{b-R}dz^+ + \int_{a+R}^{b-R}dz^-\right]\ln\frac{z-a}{z-b}, \tag{B3}$$

where dz^+ and dz^- refer to the upper (Γ_4) and lower (Γ_2) branches, respectively. Given the primitive

$$\int dz\ln(z-a) = (z-a)\ln(z-a) - z + c,$$

we find that the real part of the logarithm does not contribute to I_{2+4} (the two branches cancel out), while the imaginary part does. Indeed, choosing the branch cut of the complex log going from 0 to $+\infty$, we obtain

$$I_{2+4} = \frac{1}{2\pi}(\pi - 0 + 2\pi - \pi)(b-a) = b-a, \tag{B4}$$

which completes the derivation of Eq. (B1).

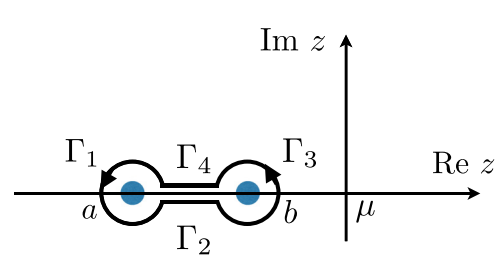

FIG. 3. Illustration of the contour used in Eq. (B1) and its decomposition in simple paths, Γ_1–Γ_4.

2. Computational evaluation of Trln terms

In order to develop a form of Eq. (17) suitable for numerical evaluation, which we have used, e.g., to make a comparison with the analytical results of this work, we follow some of the ideas from Appendix B of Ref. [26]. We start by rewriting Eq. (33) by rotating the integration over the imaginary axis:

$$\begin{aligned}\Delta E_K &= \int_{+i\infty}^{-i\infty} \frac{dz}{2\pi i} \ln\left[\frac{\det G(z)}{\det G_0(z)}\right] \qquad \text{(B5)}\\ &= \int_{-\infty}^{+\infty} \frac{dx}{2\pi} \ln\left[\frac{\det G(ix)}{\det G_0(ix)}\right]\\ &= \int_0^{+\infty} \frac{dx}{2\pi}\big[\ln\det G(ix) + \ln\det{}^* G(ix)\\ &\quad - \ln\det G_0(ix) - \ln\det{}^* G_0(ix)\big]\\ &= \int_0^{+\infty} \frac{dx}{2\pi}\big[\ln|\det G(ix)|^2 - \ln|\det G_0(ix)|^2\big]. \qquad \text{(B6)}\end{aligned}$$

In deriving these equations we have made use of the relations $G(-ix) = G(ix)^\dagger$ and $\det M^\dagger = (\det M)^*$. The last expression is suited for numerical evaluation, which we performed using a tangent grid on the imaginary axis.

3. Trln term with two interacting Green's functions

As anticipated in Sec. III B, Eq. (35) can be further generalized to the case of Trln computed for two interacting GFs, G_1 and G_2. As a first step we make reference to an arbitrary noninteracting G_0 by exploiting the identity in Eq. (19),

$$\begin{aligned}\mathrm{Tr}_\omega \ln\{G_1^{-1}G_2\} &= \mathrm{Tr}_\omega \ln\{G_0^{-1}G_2\}\\ &\quad - \mathrm{Tr}_\omega \ln\{G_0^{-1}G_1\}. \qquad \text{(B7)}\end{aligned}$$

Next, we can connect $G_{1,2}$ to G_0 via Dyson-like equations by writing

$$G_1 = G_0 + G_0(\Sigma_1 - v_0)G_1, \qquad \text{(B8)}$$

$$G_2 = G_0 + G_0(\Sigma_2 - v_0)G_2, \qquad \text{(B9)}$$

where Σ_i are suitable self-energy operators. Upon defining $\Sigma_{21} = \Sigma_2 - \Sigma_1$, the above equations give

$$G_2 = G_1 + G_1\Sigma_{21}G_2. \qquad \text{(B10)}$$

We can now evaluate Eq. (B7) by means of Eq. (35), obtaining

$$\begin{aligned}\Delta E_K &= \left[\sum_s^{\mathrm{occ}} n_s^{(2)}\epsilon_s^{(2)} - \sum^{\mathrm{occ}} \mathrm{poles}(\Sigma_2)\right]\\ &\quad - \left[\sum_s^{\mathrm{occ}} n_s^{(1)}\epsilon_s^{(1)} - \sum^{\mathrm{occ}} \mathrm{poles}(\Sigma_1)\right]. \qquad \text{(B11)}\end{aligned}$$

[1] W. Kohn, Rev. Mod. Phys. **71**, 1253 (1999).
[2] A. Pribram-Jones, D. A. Gross, and K. Burke, Annu. Rev. Phys. Chem. **66**, 283 (2015).
[3] N. Marzari, A. Ferretti, and C. Wolverton, Nat. Mater. **20**, 736 (2021).
[4] P. Hohenberg and W. Kohn, Phys. Rev. **136**, B864 (1964).
[5] R. M. Martin, L. Reining, and D. Ceperley, *Interacting Electrons Theory and Computational Approaches* (Cambridge University Press, Cambridge, 2016).
[6] E. Runge and E. K. U. Gross, Phys. Rev. Lett. **52**, 997 (1984).
[7] M. Petersilka, U. J. Gossmann, and E. K. U. Gross, Phys. Rev. Lett. **76**, 1212 (1996).
[8] C. A. Ullrich, *Time-Dependent Density-Functional Theory: Concepts and Applications* (Oxford University Press, Oxford, 2012).
[9] E. K. U. Gross, L. N. Oliveira, and W. Kohn, Phys. Rev. A **37**, 2809 (1988).
[10] T. Gould and S. Pittalis, Phys. Rev. Lett. **123**, 016401 (2019).
[11] F. Cernatic, B. Senjean, V. Robert, and E. Fromager, Top. Curr. Chem. **380**, 4 (2022).
[12] In the TD-DFT case, the variational principle takes the form of a "stationary action principle" [8].
[13] G. Stefanucci and R. van Leeuwen, *Nonequilibrium Many-Body Theory of Quantum Systems: A Modern Introduction* (Cambridge University Press, Cambridge, 2013).
[14] L. Hedin, Phys. Rev. **139**, A796 (1965).
[15] L. Reining, Wiley Interdiscip. Rev.: Comput. Mol. Sci. **8**, e1344 (2018).
[16] D. Golze, M. Dvorak, and P. Rinke, Front. Chem. **7**, 377 (2019).
[17] G. Onida, L. Reining, and A. Rubio, Rev. Mod. Phys. **74**, 601 (2002).
[18] A. L. Fetter and J. D. Walecka, *Quantum Theory of Many-Particle Systems* (McGraw-Hill, New York, 1971).
[19] J. M. Luttinger and J. C. Ward, Phys. Rev. **118**, 1417 (1960).
[20] A. Klein, Phys. Rev. **121**, 950 (1961).
[21] G. Baym and L. P. Kadanoff, Phys. Rev. **124**, 287 (1961).
[22] C.-O. Almbladh, U. von Barth, and R. van Leeuwen, Int. J. Mod. Phys. B **13**, 535 (1999).
[23] N. E. Dahlen, R. van Leeuwen, and U. von Barth, Int. J. Quantum Chem. **101**, 512 (2005).
[24] N. E. Dahlen and U. von Barth, J. Chem. Phys. **120**, 6826 (2004).
[25] N. E. Dahlen and U. von Barth, Phys. Rev. B **69**, 195102 (2004).
[26] N. E. Dahlen, R. van Leeuwen, and U. von Barth, Phys. Rev. A **73**, 012511 (2006).
[27] M. Puig von Friesen, C. Verdozzi, and C.-O. Almbladh, Phys. Rev. B **82**, 155108 (2010).
[28] S. Di Sabatino, P.-F. Loos, and P. Romaniello, Front. Chem. **9**, 751054 (2021).
[29] B. Holm and F. Aryasetiawan, Phys. Rev. B **62**, 4858 (2000).
[30] P. García-González and R. W. Godby, Phys. Rev. B **63**, 075112 (2001).
[31] T. Chiarotti, N. Marzari, and A. Ferretti, Phys. Rev. Res. **4**, 013242 (2022).
[32] M. E. Casida, Phys. Rev. A **51**, 2005 (1995).
[33] S. Kümmel and L. Kronik, Rev. Mod. Phys. **80**, 3 (2008).
[34] L. J. Sham and M. Schlüter, Phys. Rev. Lett. **51**, 1888 (1983).
[35] R. W. Godby, M. Schlüter, and L. J. Sham, Phys. Rev. B **36**, 6497 (1987).
[36] S. Ismail-Beigi, Phys. Rev. B **81**, 195126 (2010).
[37] X. Ren, P. Rinke, C. Joas, and M. Scheffler, J. Mater. Sci. **47**, 7447 (2012).

[38] J. Paier, X. Ren, P. Rinke, G. E. Scuseria, A. Grüneis, G. Kresse, and M. Scheffler, New J. Phys. **14**, 043002 (2012).

[39] M. Hellgren, N. Colonna, and S. de Gironcoli, Phys. Rev. B **98**, 045117 (2018).

[40] G. Kotliar, S. Y. Savrasov, K. Haule, V. S. Oudovenko, O. Parcollet, and C. A. Marianetti, Rev. Mod. Phys. **78**, 865 (2006).

[41] M. Gatti, F. Bruneval, V. Olevano, and L. Reining, Phys. Rev. Lett. **99**, 266402 (2007).

[42] A. Ferretti, I. Dabo, M. Cococcioni, and N. Marzari, Phys. Rev. B **89**, 195134 (2014).

[43] I. Dabo, M. Cococcioni, and N. Marzari, arXiv:0901.2637.

[44] I. Dabo, A. Ferretti, N. Poilvert, Y. Li, N. Marzari, and M. Cococcioni, Phys. Rev. B **82**, 115121 (2010).

[45] N. L. Nguyen, N. Colonna, A. Ferretti, and N. Marzari, Phys. Rev. X **8**, 021051 (2018).

[46] Y. Meir and N. S. Wingreen, Phys. Rev. Lett. **68**, 2512 (1992).

[47] H. Haug and A.-P. Jauho, *Transport and Optics of Semiconductors* (Springer, Berlin, 1996).

[48] M. B. Nardelli, Phys. Rev. B **60**, 7828 (1999).

[49] M. Brandbyge, J.-L. Mozos, P. Ordejón, J. Taylor, and K. Stokbro, Phys. Rev. B **65**, 165401 (2002).

[50] A. Calzolari, N. Marzari, I. Souza, and M. Buongiorno Nardelli, Phys. Rev. B **69**, 035108 (2004).

[51] T. Chiarotti, A. Ferretti, and N. Marzari, companion paper, Phys. Rev. Res. **6**, L032023 (2024).

[52] T. Chiarotti, Spectral and thermodynamic properties of interacting electrons with dynamical functionals, Ph.D. thesis, École Polytechnique Fédérale de Lausanne, 2023.

[53] G. E. Engel, B. Farid, C. M. M. Nex, and N. H. March, Phys. Rev. B **44**, 13356 (1991).

[54] H. N. Rojas, R. W. Godby, and R. J. Needs, Phys. Rev. Lett. **74**, 1827 (1995).

[55] S. Güttel and F. Tisseur, Acta Numerica **26**, 1 (2017).

[56] D. A. Leon, C. Cardoso, T. Chiarotti, D. Varsano, E. Molinari, and A. Ferretti, Phys. Rev. B **104**, 115157 (2021).

[57] D. A. Leon, A. Ferretti, D. Varsano, E. Molinari, and C. Cardoso, Phys. Rev. B **107**, 155130 (2023).

[58] The expression for Z_s in Eq. (13) is equivalent to $Z_s = [1 - \langle \dot{\Sigma}(\epsilon_s) \rangle]^{-1}$ when $\dot{\Sigma}$ is spatially averaged over normalized orbitals $|\phi_s\rangle = Z_s^{-1/2} |f_s\rangle$.

[59] G. Stefanucci, Y. Pavlyukh, A.-M. Uimonen, and R. van Leeuwen, Phys. Rev. B **90**, 115134 (2014).

[60] S. Y. Savrasov, K. Haule, and G. Kotliar, Phys. Rev. Lett. **96**, 036404 (2006).

[61] J. C. Budich, R. Thomale, G. Li, M. Laubach, and S.-C. Zhang, Phys. Rev. B **86**, 201407(R) (2012).

[62] L. Wang, H. Jiang, X. Dai, and X. C. Xie, Phys. Rev. B **85**, 235135 (2012).

[63] S. J. Bintrim and T. C. Berkelbach, J. Chem. Phys. **154**, 041101 (2021).

[64] S. J. Bintrim and T. C. Berkelbach, J. Chem. Phys. **156**, 044114 (2022).

[65] R. A. Brualdi and H. Schneider, Linear Algebra Its Appl. **52–53**, 769 (1983).

[66] F. Aryasetiawan, T. Miyake, and K. Terakura, Phys. Rev. Lett. **88**, 166401 (2002).

[67] S. Y. Savrasov and G. Kotliar, Phys. Rev. B **69**, 245101 (2004).

[68] In principle the condition $\Omega^2 > \max_s \epsilon_s^2$ would be enough to guarantee the thesis.

[69] P. W. Anderson, Phys. Rev. **124**, 41 (1961).

[70] K. Yosida and K. Yamada, Prog. Theor. Phys. Suppl. **46**, 244 (1970).

[71] K. Yamada, Prog. Theor. Phys. **53**, 970 (1975).

[72] B. Horvatić, D. Sokcević, and V. Zlatić, Phys. Rev. B **36**, 675 (1987).

[73] E. Kozik, M. Ferrero, and A. Georges, Phys. Rev. Lett. **114**, 156402 (2015).

[74] R. Eder, arXiv:1407.6599.

[75] A. Stan, P. Romaniello, S. Rigamonti, L. Reining, and J. A. Berger, New J. Phys. **17**, 093045 (2015).

[76] R. Rossi and F. Werner, J. Phys. A **48**, 485202 (2015).

[77] T. Schäfer, S. Ciuchi, M. Wallerberger, P. Thunström, O. Gunnarsson, G. Sangiovanni, G. Rohringer, and A. Toschi, Phys. Rev. B **94**, 235108 (2016).

[78] W. Tarantino, P. Romaniello, J. A. Berger, and L. Reining, Phys. Rev. B **96**, 045124 (2017).